Review

Advanced Nb$_2$O$_5$ Anode towards Fast Pseudocapacitive Sodium Storage

Qinglin Deng [1,2,*] and **Lingmin Yao** [1,2,*]

1 School of Physics and Materials Science, Guangzhou University, Guangzhou 510006, China
2 Research Center for Advanced Information Materials (CAIM), Huangpu Research & Graduate School, Guangzhou University, Guangzhou 510555, China
* Correspondence: qldeng@gzhu.edu.cn (Q.D.); lingminyao@gzhu.edu.cn (L.Y.)

Abstract: Intercalation-type Nb$_2$O$_5$, based on its inherent structural advantages in energy storage, shows excellent energy storage characteristics in sodium-ion batteries (SIBs). The rapid pseudocapacitive Na-ion insertion/extraction dynamic mechanisms result in its outstanding rate performance. However, the inherent low electronic conductivity hinders its application and development in SIBs. Though various modification projects can effectively ameliorate these shortcomings, there are also some basic research problems that need to be clarified and solved. This review summarizes the latest research progress of Nb$_2$O$_5$ in SIBs. The structural advantages and pseudocapacitive characteristics of sodium storage are emphasized. The recent advanced modification strategies are summarized comprehensively, including carbon modification, structural optimization, defect engineering, increased mass loading, flexible electrodes, synergistic effect electrodes, etc. In addition, this review summarizes and prospects the key research strategies and future development directions of Nb$_2$O$_5$ in future practical applications.

Keywords: Nb$_2$O$_5$; anode; sodium ion batteries; pseudocapacitive; intercalation-type

1. Introduction

1.1. Battery Technology

Energy and environment are the foundation of human survival and development and determine the sustainable development of human society [1]. Solar energy, wind energy, tidal energy, hydrogen energy and other green energies have been widely considered [2–6]. However, these energy sources are affected by regional conditions and have the characteristics of localization, randomness, regionality and intermittency, resulting in huge restrictions on their use. The key to solve this problem is to develop efficient energy storage and energy conversion devices to collect these scattered energies [7,8]. Among them, the energy storage secondary battery is one of the most effective and promising energy storage devices [9–11].

As the typical representative of energy storage capacity, lithium-ion batteries (LIBs) have been widely used with lots of advantages [12,13]. The growing electronic product and new energy vehicle market in the future will demand LIBs in an unprecedented manner, which will inevitably lead to a shortage of lithium resources and rising costs [14]. Additionally, global lithium resources are scarce. The abundance of lithium in the earth's crust is only about 0.0017%, and the distribution is uneven. The recycling mechanism of LIBs is not yet mature, which further restricts their extensive application in the future [15]. Therefore, it is urgent to develop energy storage secondary batteries with abundant resources and low prices. Among them, sodium-ion batteries (SIBs) have received special attention [16–18]. Table 1 shows the characteristics, advantages and disadvantages of LIBs and SIBs. Sodium and lithium belong to the same main group, and their physical and chemical properties are similar. However, the reserves of sodium on the earth are up to 2.3%, which is much more than lithium. Moreover, they are widely distributed, rarely limited by regions. In

addition, for the electrolyte with the same concentration, the ion conductivity of sodium ion electrolyte is higher than that of lithium ion, so we can choose a lower concentration of sodium ion electrolyte, which can also reduce the cost. Since sodium does not form an alloy with aluminum, aluminum foil can be used as the current collector for the negative electrode, which can further reduce the cost. It can be seen that SIBs will show a huge cost advantage in the future with smart grids and large-scale energy storage systems [17,19,20].

Table 1. Characteristics, advantages and disadvantages of LIBs and SIBs.

	LIBs	**SIBs**
Battery structure	Similar	Similar
Ionic radius	0.076 nm (Li)	0.102 nm (Na)
Voltage vs. SHE	-3.04 V (Li)	-2.71 V (Na)
Crust Abundance	0.0017 mass % (Li)	2.3 mass % (Na)
Advantages	1. High energy density 2. Mature technology 3. Long cycle life 4. Small size and light weight	1. Rich Na reserves 2. Al foil can be used as the collector for anode 3. Lower concentration of electrolyte is allowed
Disadvantages	1. Lithium dendrite problem 2. Scarce Li reserves and high production cost	1. Low energy density 2. Immature technology 3. Poor cycle life

1.2. Anodes of Sodium-Ion Batteries

In terms of structure, SIBs are mainly composed of cathode, anode, separator, electrolyte, current collector, battery shell, etc. Among them, cathode and anode active materials play a decisive role in battery performance. The function of the separator is to prevent short circuit and allow sodium ions to pass through. The commonly used separator is glass fiber membrane. Common electrolytes include sodium perchlorate, sodium hexafluorophosphate, sodium tetrafluoroborate, etc. Generally, carbonic ester or ether will be used as solvent. Since Na and Al do not form an alloy, aluminum foil can be used as the current collector for both the cathode and anode electrodes. The sodium storage mechanism for SIBs is schematically depicted in Figure 1. Similar to LIBs, anode and cathode active materials directly affect various energy storage performances, including specific capacity, rate, cycle and safety performances [21–23]. According to the different sodium storage mechanisms, the anode electrode of SIBs can be divided into three types: alloy-type, conversion-type and intercalation-type [21,24–26]. Alloy-type anode materials will undergo an alloying reaction in the process of sodium storage. They have high theoretical specific capacity and a low working voltage platform. At present, they are mainly composed of Ge, Sn, P, Sb, etc. [24,27–29]. However, due to the inherent defects of alloy materials, large sodium ion radius in the alloy/dealloying reaction process will lead to huge volume changes.

The conversion-type electrode materials will undergo phase transition during the charge/discharge process. Some anode materials will undergo an alloying reaction after the first conversion reaction [30,31]. The theoretical specific capacity of the conversion-type anode is high. However, it also faces various shortcomings, such as low Coulomb efficiency of the first lap, poor rate dynamics, etc. In addition, the electrode will also undergo large volume expansion in the conversion reaction process, resulting in the progressive pulverization of active materials and eventually leading to the decline of capacity and cycle stability [25,32].

Different from the sodium storage mechanism of alloy-type and conversion-type, the intercalation-type anode is based on the intercalation mechanism. Most electrode materials have low theoretical specific capacity, but with negligible volume change during the charging and discharging process, showing excellent rate and cycling performance. At present, the typical intercalation-type anode materials for SIBs are mainly composed of

carbon-based materials [33–35], titanium-based oxides (such as TiO_2, $Na_2Ti_3O_7$) [36,37], niobium-based oxides (such as Nb_2O_5, $TiNb_2O_7$, $Ti_2Nb_2O_9$), etc. [26,38–40]. Although the volume expansion effect of some oxide anodes is small when storing sodium, their intrinsic electronic conductivity is poor, which also significantly affects the release of their excellent rate and cycle stability performances.
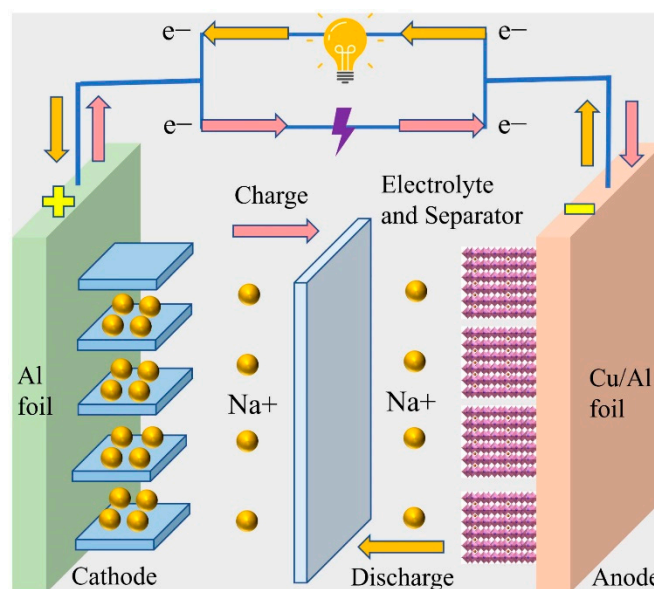

Figure 1. Schematic illustration of sodium storage mechanism for SIBs.

1.3. Intercalation-Type Nb_2O_5 Anode

Different sodium storage anodes have their own advantages and disadvantages in energy storage. The theoretical specific capacities of alloy-type and conversion-type are higher, but the rate and cycle stability performances are poor. On the contrary, the theoretical specific capacity of the intercalation-type is lower, but the rate and cycle stability performances are better [21]. With the extensive use of electronic products in the future and the improvement of user experience, higher requirements are put forward for the demand in energy and power density of batteries. Especially for the current fast charging market, on the premise of the existing battery energy density, the improvement of charging and discharging speed will be conducive to the maximum use of the product and enhance the user experience. Among the intercalation-type anodes of SIBs, the niobium-based oxide anodes, especially for Nb_2O_5-based electrodes, are raising more attention based on their inherent structural energy storage advantages [38,41,42]. Nb_2O_5-based anodes have been widely used in LIBs, accompanied by excellent rate and cycle stability performances [43–45]. At present, more and more researchers pay attention to their application in SIBs and in doing so reveal the relevant sodium storage mechanisms.

As far as we know, there are few comprehensive reviews on Nb_2O_5 electrodes for application in SIBs. Compared with previous similar work [42], they basically focus on reviewing the niobium-based oxide family in LIBs and SIBs, making the research on Nb_2O_5 in SIBs difficult to centralize. This paper will directly and systematically review intercalation-type Nb_2O_5 anodes for application in SIBs with the latest research progresses, which were mainly published from 2018 to 2022. Figure 2 shows the energy storage characteristics and modification strategies of Nb_2O_5 in SIBs. We comprehensively analyzed the structural advantages of Nb_2O_5 in sodium storage and the disadvantages of low electronic conductivity. Moreover, based on the latest published literature, in addition to some important concerns and prospects such as carbon modification, structural optimization and defect engineering, this review will also outline Nb_2O_5 anodes in SIBs from a novel perspective, including the mass loading effect, flexible electrodes and synergistic effect electrodes, which can effectively improve its energy storage performances and extend its practical application

fields. In addition, we also expound on the opportunities and challenges of Nb_2O_5 in future practical applications and commercialization.
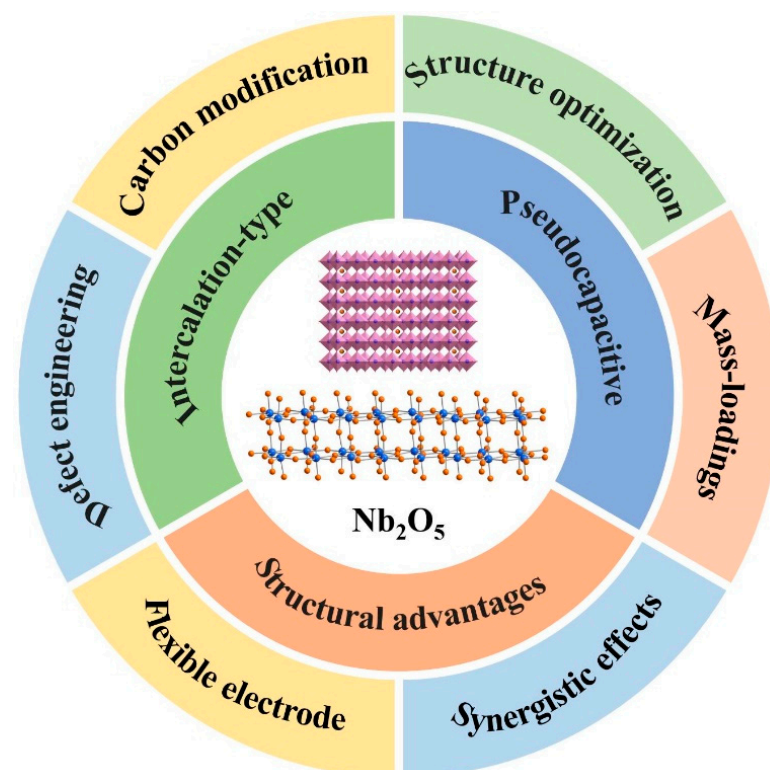

Figure 2. Energy storage characteristics and modification strategies of Nb_2O_5 in SIBs.

2. Energy Storage Structure of Nb_2O_5 Anode

According to different heat treatment conditions, Nb_2O_5 has several crystal forms, such as T-Nb_2O_5, B-Nb_2O_5 and H-Nb_2O_5 [46]. These different crystal structures greatly affect their respective electrochemical energy storage performances. Among them, T-Nb_2O_5 with an orthorhombic crystal phase shows significantly better energy storage performance. T-Nb_2O_5 has a *Pbam* space group, and its XRD crystal phase matches JCPDS card No. 30-0873. The Nb ions in the lattice are surrounded by six or seven O ions, forming a polyhedron of NbO_6 and NbO_7 with shared twisted edges/corners [47]. As shown in Figure 3, according to the atomic arrangement of T-Nb_2O_5, its crystal structure can be seen as two alternating atomic layers, including a loosely packed 4 g layer and a dense 4 h layer [48]. Because the 4 g layer has a spacious atom holding space, it can provide preferred storage and transportation sites for ions [48].

T-Nb_2O_5 has been widely used as the anode of LIBs, showing excellent rate and cycle stability performances, accompanied by ultra-fast pseudocapacitive lithium-ion storage dynamics. The rapid lithium ion insertion/extraction mechanism occurs not only on the surface, but also in bulk materials [48,49]. Although the ionic radius of Na-ion (0.102 nm) is larger than that of Li-ion (0.076 nm), a larger ionic radius may lead to larger volume expansion and slower sodium storage kinetics. However, based on the inherent structural advantages, the 0.39 nm large crystal plane spacing of the (001) plane in T-Nb_2O_5 can accommodate a certain amount of Na-ion, so it can be used as a potential anode material for SIBs. The sodium insertion/extraction reaction mechanism of Nb_2O_5 electrode can be summarized by the following equation: $Nb_2O_5 + xNa^+ + xe^- \Leftrightarrow Na_xNb_2O_5$, x is the mole fraction of the inserted Na-ions [38].

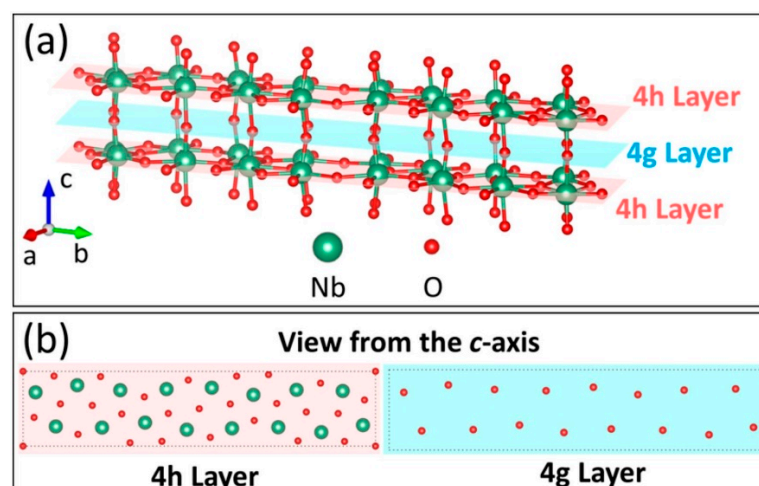**Figure 3.** (**a**) Structure of T-Nb$_2$O$_5$ with highlighted 4 h layers. (**b**) Atomic arrangements of the 4 h layer and the 4 g layer when viewed from the *c*-axis view. Reprinted with permission from Ref. [48] Copyright 2017 American Chemical Society.

3. Pseudocapacitive Energy Storage Mechanisms

The intercalation-type Nb$_2$O$_5$ electrodes are based on the intercalation mechanism, which means that sodium ions are embedded into the lattice or layer spacing of the material to form a stable sodium intercalation compound without affecting the lattice parameters of the material. As the sodium ions mostly occupy the lattice and gap positions of the material during the intercalation process, significant expansion changes in the overall structure of the material can be avoided. Therefore, the intercalation-type Nb$_2$O$_5$ anode has excellent structural stability and cycling performance. However, due to the limitation of the gap position, its theoretical specific capacity is usually relatively low.

For SIBs, the large sodium ion radius will lead to slow ion diffusion dynamics and large volume expansion in the process of insertion/extraction, which seriously restricts their rate performance. The intercalation-type Nb$_2$O$_5$ anodes have unique pseudocapacitive energy storage features due to their inherent structural advantages [48,49]. Because there are more positions for ion storage between layers, sodium ions can be inserted and extracted more easily. Pseudocapacitive electrode materials have excellent reaction reversibility, showing similar electrochemical characteristics to capacitors [50,51]. At present, pseudocapacitive mechanisms can be divided into three categories from the electrochemical perspective: underpotential deposition, surface redox pseudocapacitive and intercalation pseudocapacitive [51]. As shown in Figure 4, for the surface redox pseudocapacitive, the storage of sodium ions only occurs in a limited area near the surface, accompanied by a Faraday charge transfer process [52]. For intercalation pseudocapacitive, sodium ions in electrode active materials can conduct rapid ion transport along diffusion channels of all dimensions without phase transition. From the view of dynamics, measuring the response current of energy storage electrode materials at different scanning rates is the most appropriate tool to distinguish battery type (diffusion control) or capacitance (surface control). The studying of pseudocapacitive features is mainly based on the cyclic voltammetry (CV) curve of the electrode with variable sweep rate [53,54].

As we know, the CV curves follows the power-law relationship [55]:

$$i = av^b \tag{1}$$

where *a* and *b* are adjustable parameters, *i* is the current, and *v* is the sweep rate. Equation (1) can be equally converted to Equation (2).

$$\log(i) = \log(a) + b\log(v) \tag{2}$$

The *b* value can reflect the intrinsic charge storage kinetics. It is close to 0.5 and 1, which indicate the diffusion-controlled redox reaction and surface-controlled pseudocapacitive storage reaction, respectively [52]. Moreover, *i* can be divided into two parts at a fixed potential (V). It can be expressed as Equation (3).

$$i(\text{V}) = k_1 v + k_2 v^{1/2} \tag{3}$$

where $k_1 v$ and $k_2 v^{1/2}$ represent surface-controlled capacitance and diffusion-controlled reactions, respectively. Equation (3) can be rearranged to Equation (4).

$$i(\text{V})/v^{1/2} = k_1 v^{1/2} + k_2 \tag{4}$$

The curves of Equation (4) can be plotted at a fixed potential with various sweep rates. The calculated slope and *y*-intercept are k_1 and k_2, respectively. The current values of capacitive contribution parts at different potentials are obtained using $k_1 v$, then the contribution ratio of capacitance and diffusion can be obtained [38]. Based on the inherent structural energy storage advantages of intercalation-type Nb_2O_5 anodes, they show the fast Na-ion pseudocapacitive storage features. The above CV research methods can be used to investigate the Na-ion storage mechanism of Nb_2O_5-based anodes, which is a surface-controlled pseudocapacitive or a diffusion-controlled behavior, then further obtain the corresponding contribution ratio. In addition, Zhang et al. have revealed the electrochemical sodium storage mechanism of orthogonal-Nb_2O_5 nanosheets using in situ transmission electron microscopy [56].
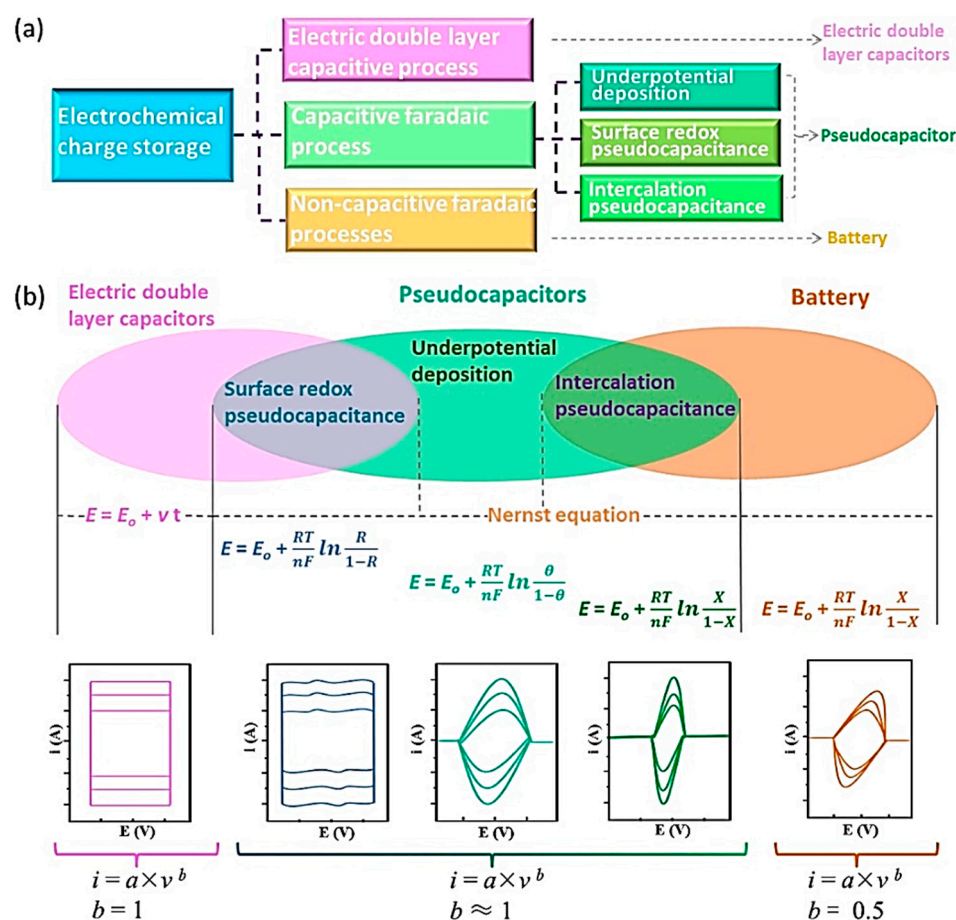

Figure 4. (**a**) Different types of electrochemical charge storage processes. (**b**) Schematic illustration of correlations and differences among these electrochemical processes. Reprinted with permission from Ref. [52] Copyright 2019 Elsevier.

4. Applications in Sodium-Ion Batteries

The application of T-Nb_2O_5 electrodes in SIBs is limited due to their poor intrinsic conductivity (~3.4 × 10^{-6} S cm^{-1} at 300 K) [42]. Structure optimization and surface engineering are often used to improve the energy storage of electrode materials [41,57–61]. An ideal modified electrode structure requires the ability to effectively improve the conductivity of the material, buffer volume expansion and increase the contact area with the electrolyte.

4.1. Carbon Modification

Due to the poor intrinsic electronic conductivity of the Nb_2O_5 electrode, its application in SIBs is limited, which is one of the most important problems that need be solved for this material. Poor electronic conductivity will greatly affect the high-rate performance and cycle stability of Nb_2O_5. An effective method is to composite Nb_2O_5 with carbon materials to improve the electronic conductivity. As shown in Figure 5, Zhou et al. prepared nanocomposites of carbon-decorated T-Nb_2O_5 nanocrystals anchored on rGO nanosheets (T-Nb_2O_5-C-rGO) [62]. They have a high reversible specific capacity of 240 mA h g^{-1} under the current density of 0.1 A g^{-1}, with a good cycle stability with 68% capacity retained at 1 A g^{-1} after 1000 cycles. With the aid of the three-dimensional porous rGO fiber structure and carbon coating layer, the electronic conductivity of the composite was significantly improved, resulting in the excellent sodium storage performance. Moreover, Liu et al. designed an N-doped carbon-coated urchin-like Nb_2O_5 nanoarchitecture (Nb_2O_5@C) [63]. Such structure can decrease the diffusion pathway of ions and electrons. It can also improve the electronic conductivity and buffer the volume expansion. As a result, this electrode presented excellent rate and cycle stability performances in SIBs. It has a higher reversible specific capacity of 255 mA h g^{-1} under the current density of 1 A g^{-1} over 150 cycles with a Coulombic efficiency approaching 100%, which is much better than Nb_2O_5 (94 mA h g^{-1} with a Coulombic efficiency of about 82%). When the current density increases to 10 A g^{-1}, it still shows a high reversible specific capacity of 160 mA h g^{-1} over 1000 cycles. In addition, ultrasmall Nb_2O_5 nanoparticles wrapped with nitrogen-doped carbon were synthesized by Yu et al. [64] They show an outstanding cycling stability with a high reversible specific capacity of 128.4 mA h g^{-1} and 95.9 mA h g^{-1} after 3000 cycles under high current densities of 5 A g^{-1} and 10 A g^{-1}, respectively. The enhanced sodium storage performance can be attributed to the improved electronic conductivity, relief of stress and shortening of ion and electron transmission distance.

Graphene is often used as a modifier based on its excellent electronic conductivity. Li et al. prepared uniform sandwich-like mesoporous Nb_2O_5/graphene/mesoporous Nb_2O_5 nanosheets as the anode for SIBs [65]. Sun et al. prepared Nb_2O_5 nanowires@PECVD-derived graphene anode [66]. Both of them demonstrated excellent sodium storage performances with the aid of graphene, along with improved electronic conductivity. Yu et al. prepared S-doped T-Nb_2O_5 hollow nanospheres/S-doped graphene networks [67]. Owing to the effects of S-doping and the excellent electronic conductivity of graphene, the sodium storage performance of T-Nb_2O_5 was dramatically improved. It demonstrated a high specific capacity of 100 mA h g^{-1} at 20C rate after 3000 cycles. In addition, other carbon-modified samples, such as Nb_2O_5 nanoparticles/N-doped graphene hybrid anode [68], carbon-confined ultrasmall T-Nb_2O_5 nanocrystals anchored on a carbon nanotube electrode [69], mesoporous niobium pentoxide/carbon composite electrode [70], pomegranate-like structured Nb_2O_5/carbon@N-doped carbon composites [71], core-shell structured Nb_2O_5@N-doped carbon nanoparticles [72], etc., all delivered excellent rate and cycle stability performances.
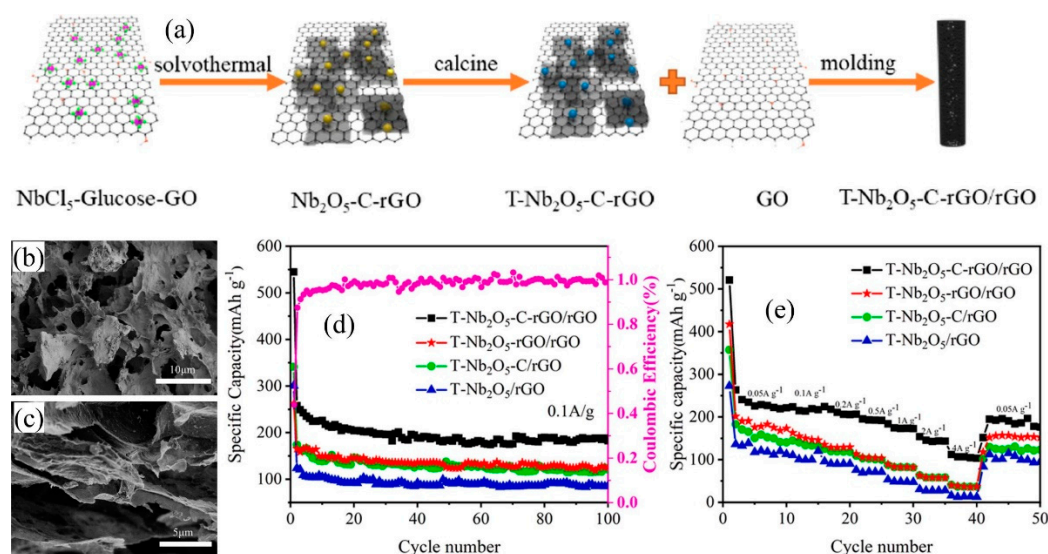
Figure 5. (**a**) Schematic of the fabrication procedure for T-Nb$_2$O$_5$-C-rGO/rGO fiber anode. Cross-sectional scanning electron microscopy images of T-Nb$_2$O$_5$-C-rGO/rGO fiber (**b**) before pressing and (**c**) after pressing. (**d**) Cycling performance and (**e**) rate performance of samples. Reproduced with permission from Ref. [62] Copyright 2022 Elsevier.

4.2. Structure Optimization

The combination of nanostructures and carbon modification can effectively enhance ion transport kinetics. Hu et al. prepared carbon-bridged Nb$_2$O$_5$ mesocrystals by a rapid microwave-assisted method and subsequent heat treatment [73]. Carbon coating/bridging can improve electronic conductivity. The designed mesocrystalline structure possesses rich boundaries and a uniform nanocrystalline orientation. Supported by these structural advantages, the electrode shows ultrafast sodium storage performances. It shows a high specific capacity of 133.4 mA h g^{-1} under a high current density of 50 C (72 s). The electrode also exhibits excellent cycle stability with a high retention of 80.5% (112.4 mA h g^{-1}) after 10,000 cycles at the high current density of 20 C. Moreover, the galvanostatic intermittent titration technique (GITT) results indicate that the well-defined mesocrystalline architecture dramatically shorten the Na-ion transport distance and promotes the intercalation behavior of Na-ions. As we know, during the charging and discharging process, the crystalline phase of the Nb$_2$O$_5$ electrode will change to amorphous, limiting its electrochemical sodium storage performance. Aiming at this problem, Li et al. designed a 3D ordered macroporous amorphous Nb$_2$O$_5$ with rich mesoporosity [74]. The hierarchical porous structure promotes the insertion and extraction of sodium ions. As the anode of SIBs, it shows good sodium storage performances with a high specific capacity of 131 mA h g^{-1} after 500 cycles at the current density of 5 A g^{-1}. In addition, owing to the effective structural regulation strategies of nanowires and quantum dots, architecturing aligned orthorhombic Nb$_2$O$_5$ nanowires and Nb$_2$O$_5$ quantum dots confined in multi-chamber yeast carbon also exhibit excellent energy storage performance in SIBs [75,76].

4.3. Defect Engineering

Nanoscale defect engineering has been widely used to improve the energy storage performance of electrodes [77,78]. As shown in Figure 6, Chen et al. designed a Nb$_2$O$_5$@carbon nanoreactor containing both an O–Nb–C heterointerface and oxygen vacancies (Nb$_2$O$_{5-x}$@MEC) [79]. This nanoreactor not only effectively immobilizes defective Nb$_2$O$_5$ by forming an O-Nb-C heterointerface, but also provides uniform dispersion of Nb$_2$O$_5$ to prevent their agglomeration. The framework is favorable to improve sodium storage and enhance redox reaction kinetics. Benefiting from such structural advantages, as the anode of SIBs, it presents a high discharge specific capacity of 450, 325, 250, 215, 192, 179,

156 and 130 mA h g^{-1} at 0.2, 0.4, 1, 2, 4, 6, 10 and 20 A g^{-1}, respectively. Even under a high current density of 20 A g^{-1}, it still has reversible specific capacity of 105 mA h g^{-1} with stable Coulombic efficiency of nearly 100% after 5000 cycles. Moreover, Lee et al. prepared partially surface-amorphized and defect-rich black Nb$_2$O$_{5-x}$@graphene nanosheets with the aid of surface-engineering treatment [80]. The sample shows lots of defects including Nb^{4+} ions, oxygen vacancies and an amorphous surface layer, which bring improved electron transport and enhanced surface capacitance energy storage. As a result, the electrode delivers excellent rate performance with a high specific capacity of 202 and 123 mA h g^{-1} at the current densities of 500 and 3000 mA g^{-1}, respectively.
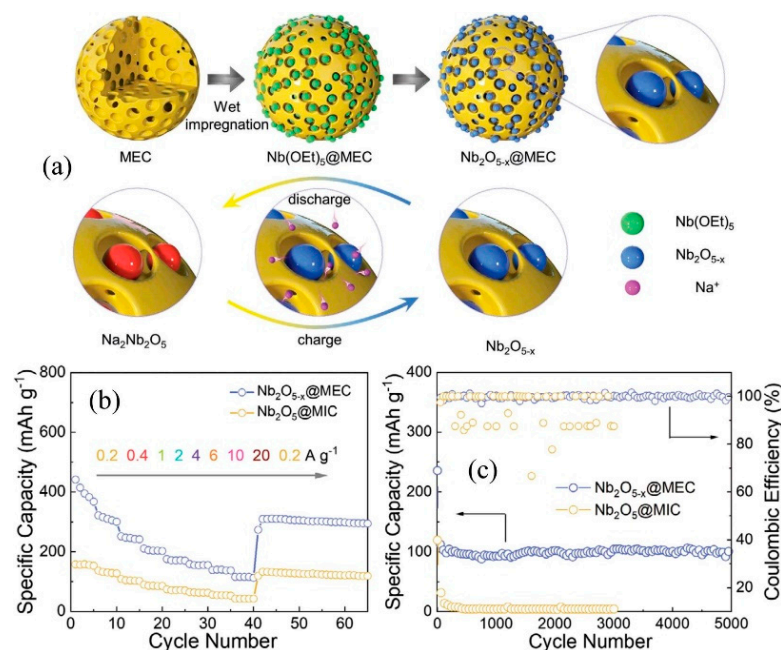

Figure 6. (**a**) Schematic illustration of the synthetic procedure of Nb$_2$O$_{5-x}$@MEC composites. (**b**) Rate performance and (**c**) long-term cycling performance under the current density of 20 A g^{-1} of Nb$_2$O$_{5-x}$@MEC electrode. Reproduced with permission from Ref. [79] Copyright 2022 Wiley.

4.4. Increased Mass Loading

As we know, through structural optimization and carbon modification engineering, the sodium storage performance of Nb$_2$O$_5$ electrode can be effectively improved. However, most of the reported electrodes are based on low mass loading of active materials. In order to maximize the energy density of batteries, commercial secondary batteries put forward higher requirements on the mass loading of active electrode materials. Although the electrode with low mass loading has obvious advantages in the transport of ions and electrons, its practical application is limited. Especially for SIBs, developing an effective electrode structure with excellent sodium storage performance under high mass loading is crucial for future commercial applications. Duan et al. made a major breakthrough in the research of using the high mass loading of Nb$_2$O$_5$ electrode in LIBs [43]. It was found that three-dimensional porous graphene can be used as a frame structure to achieve high mass loading of electrode materials. The research also optimized the rate performance and area capacity of the electrode at high mass loading, which indicates that the Nb$_2$O$_5$ composite electrode shows great potential in commercial application. For its sodium storage applications, as shown in Figure 7, Cao et al. designed a 3D porous network composed of carbon nanotube (CNT)@T-Nb$_2$O$_5$@C nanocables [81]. In this structure, an Nb$_2$O$_5$ intermediate layer is sandwiched between an underlying CNT skeleton and an outer carbon shell. By thickening the Nb$_2$O$_5$ intermediate layer, the mass loading of a sponge anode can be effectively improved. As the anode of SIBs, the sponge electrode shows reversible areal capacities of 2.7 mA h cm^{-2} after 200 cycles when the mass loading

reaches 16.6 mg cm^{-2} with a negligible capacity fading rate. Such performance is more than 9 times better than the previously reported Nb_2O_5-based samples.
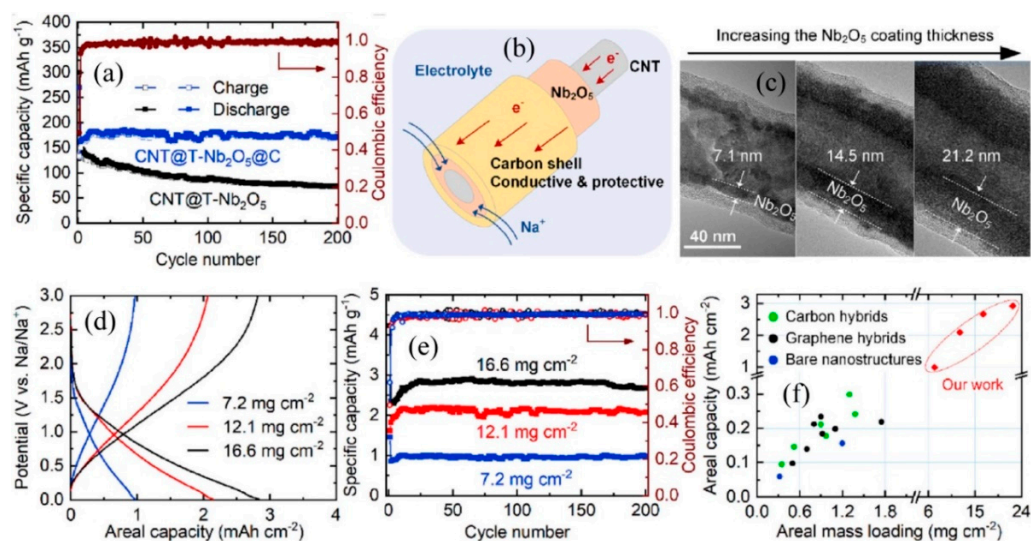

Figure 7. (**a**) Cycling performance of the CNT@T-Nb_2O_5@C and CNT@T-Nb_2O_5 electrode at a current density of 100 mA g^{-1}. (**b**) Schematic showing the electrochemical process within the sponge electrode. (**c**) TEM images of the CNT@T-Nb_2O_5@C sponge electrode with increasing thicknesses. (**d**) The discharge/charge voltage profiles at 50th cycle of the sponge electrodes with different areal mass loadings. (**e**) Cycling performance of the sponge electrodes with different areal mass loadings. (**f**) Literature survey on the areal mass loadings and capacities of the reported Nb_2O_5-based structures for sodium storage. Reproduced with permission from Ref. [81] Copyright 2020 Elsevier.

4.5. Flexible Electrode

Flexible electronic devices have important application prospects in biological, medical, display, wearable health devices and other fields [82–84]. Accordingly, it is necessary to develop flexible power supply devices. Therefore, the development of flexible energy storage electrodes is one of the most critical steps for the wide application of flexible electronic devices. In addition, the active material of the electrode is usually loaded on a heavy metal collector. If taking the weight of the metal collector into account, the specific capacity of the entire electrode is much smaller [85]. Therefore, the development of free-standing, adhesive-free, conductive agent-free and metal collector-free flexible electrodes can effectively improve the energy density of the entire battery. Based on the rapid sodium-ion insertion/extraction kinetics of Nb_2O_5, developing flexible Nb_2O_5 sodium storage anodes will have an important application prospect.

As shown in Figure 8, Hu et al. designed large-area free-standing mesoporous T-Nb_2O_5/carbon nanofiber films (m-Nb_2O_5/CNF) via an electrospinning method [86]. In this structure, polyacrylonitrile is used as a carbon source and flexible support frame after carbonization. Tetraethyl orthosilicate is a template precursor. Mesoporous networks are obtained after thermal treatment of the precursor nanofibers and subsequent SiO_2-etching. As the anode of SIBs, the m-Nb_2O_5/CNF film electrode delivers a high specific capacity of 287 mA h g^{-1} and 172 mA h g^{-1} at the rates of 0.5 C and 150 C, respectively. By applying electrospinning technology, Liu et al. also fabricated flexible Nb_2O_5 nanorods/microporous multichannel carbon nanofiber film anode [87]. It shows a high specific capacity of 287 mA h g^{-1} at 4 A g^{-1} and a high retention of 91% after 10,000 cycles at 2 A g^{-1}. Moreover, carbon cloth is also often used as a flexible self-supporting framework. Chen et al. investigated the sodium storage application of Nb_2O_5 nanotubes on carbon cloth [88]. In addition, Cao et al. prepared a flexible Nb_2O_5/carbon nanotube film through a facile hydrothermal treatment and vacuum filtration process [89]. With the aid of multiwalled carbon nanotubes and vacuum filtration, Zanin et al. also obtained a

free-standing Nb_2O_5-based sodium storage anode [90]. In addition, Yu et al. designed 3D porous reticular T-Nb_2O_5@carbon thin film electrodes via an electrostatic spray deposition technique, showing excellent rate and cycle stability performances [91]. As we can see, selecting appropriate preparation technology is an effective way to prepare self-standing electrodes.
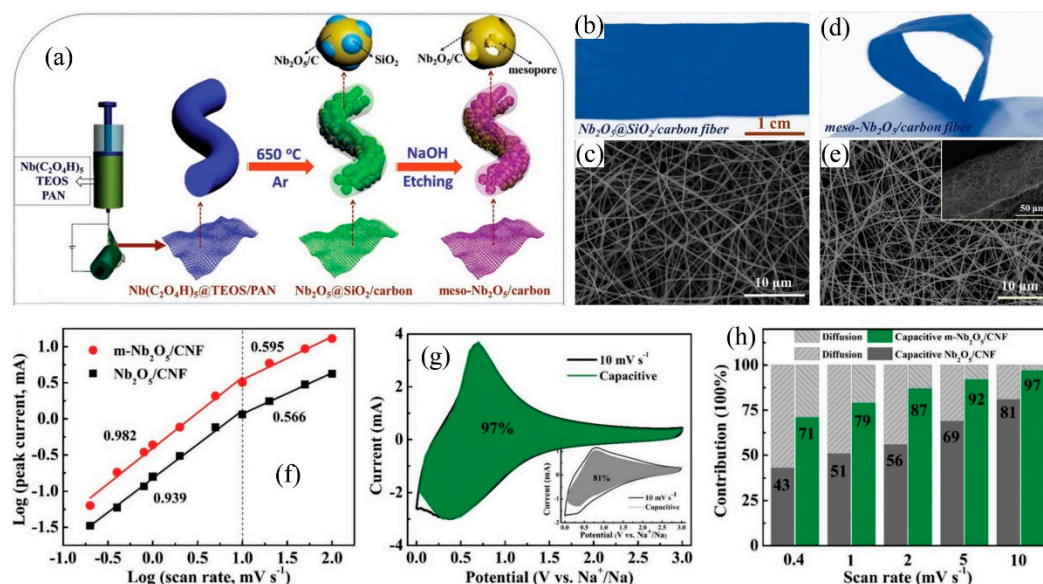

Figure 8. (**a**) Schematic illustration of the fabrication of flexible m-Nb_2O_5/CNF films. Photograph and SEM images of (**b,c**) Nb_2O_5/SiO_2/CNF and (**d,e**) m-Nb_2O_5/CNF. (**f**) The relationship between peak currents and scan rates of m-Nb_2O_5/CNF and Nb_2O_5/CNF. (**g**) Capacitive contribution curves of m-Nb_2O_5/CNF at 10 mV s^{-1}. (**h**) Normalized ratio for m-Nb_2O_5/CNF and Nb_2O_5/CNF at different scan rates. Reproduced with permission from Ref. [86] Copyright 2019 Wiley.

4.6. Electrode Based on Synergistic Effects

Structural engineering, defect engineering and carbon modification strategies have been widely used to solve Nb_2O_5's poor conductivity and improve its sodium storage performance. Lots of remarkable achievements have been achieved [38]. The flexible electrode strategy is also expected to significantly improve the energy density of the entire battery [92]. Although these modification projects can effectively improve the sodium storage performance, the relatively low theoretical specific capacity still limits the practical application of Nb_2O_5 in SIBs. Based on the inherent structural advantages, the intercalation-type Nb_2O_5 shows a rapid sodium insertion/extraction behavior and excellent cycle stability performance. In order to give full play to the energy storage advantages of Nb_2O_5 and make up for its relatively low specific capacity of sodium storage, an effective strategy is to composite alloy-type or conversion-type anodes, which have higher theoretical specific capacity but poor rate and cycle stability performances. With the aid of multiple mechanism synergetic effects, the composite electrodes will give play to their respective energy storage advantages of different anode materials and complement their respective energy storage disadvantages, which can effectively improve the specific capacity, rate and cycle performances of SIBs.

As shown in Figure 9, by subtly utilizing the synergistic effect of three different sodium storage mechanisms, including the intercalation-type Nb_2O_5, conversion-type MoS_2 and adsorption-type hard carbon, Zhu et al. designed a three-dimensional flexible Nb_2O_5@hard carbon@MoS_2@Soft carbon composite electrode material [93]. The hard carbon network derived from electrospinning provides a flexible support framework. Intercalation-type Nb_2O_5 has the inherent advantage of sodium storage, showing excellent rate and cycle stability performance. The recombination of MoS_2 significantly improves the specific capacity of the electrode and therefore constructs a Nb_2O_5@MoS_2 heterojunction channel

with enhanced sodium transport. The coated soft carbon not only improves the electronic conductivity, but also restrains the volume expansion of the electrode. The sodium storage capacity of the prepared composite electrode is higher than that of hard carbon and Nb_2O_5, and the rate and cycling performance are better than MoS_2. After 20,000 cycles, the capacity maintenance rate is still more than 82%. Such excellent performance can be attributed to the beneficial integration of multiple mechanisms in adsorption, intercalation and conversion, as well as the accompanying multiple synergistic effects. In particular, Nb_2O_5 with fast pseudocapacitive sodium storage behavior plays an important role in enhancing the electrochemical sodium storage performance of this composite electrode [93]. In addition, alloy-type antimony (Sb) anode shows a high theoretical capacity of 660 mA h g^{-1} for SIBs, but with a poor rate performance. Based on the energy storage advantages and disadvantages of Nb_2O_5 and Sb, Bi et al. prepared $Sb-Nb_2O_5$ nano-meshes [94]. As for the application in SIBs, they show a high specific capacity of 190 mA h g^{-1} at the current density of 10 A g^{-1} under the accompanying synergistic effect. Table 2 shows the energy storage performances of the reported Nb_2O_5-based and other typical intercalation-type anode materials for application in SIBs.
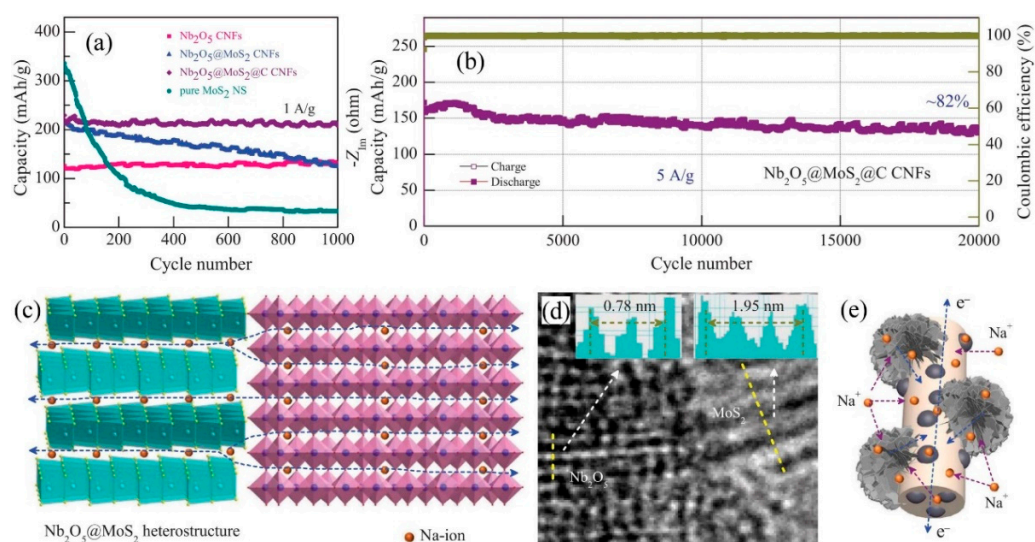

Figure 9. (**a**) Cycling stability of samples at a current density of 1 A g^{-1}. (**b**) Cycling stability of $Nb_2O_5@MoS_2@C$ CNFs electrode at a high current density of 5 A g^{-1}. (**c**) One kind of the heterointerface of $Nb_2O_5@MoS_2$ with (**d**) the corresponding TEM image. (**e**) The possible sodium storage mechanism. Reproduced with permission from Ref. [93] Copyright 2020 Wiley.

Table 2. Energy storage performances of the reported Nb_2O_5-based and other typical intercalation-type anode materials for application in SIBs.

Materials	Sodium Storage Performances	References
$Nb_2O_5@NC$	128.4 mA h g^{-1} and 95.9 mA h g^{-1} after 3000 cycles at 5 A g^{-1} and 10 A g^{-1}, respectively.	[64] Nanoscale, 2020, 12, 18673
$Nb_2O_5@C$	255 mA h g^{-1} at 1 A g^{-1} over 150 cycles, and 160 mA h g^{-1} at 10 A g^{-1} over 1000 cycles	[63] J. Mater. Chem. A, 2021, 9, 23467
T-Nb_2O_5-C-rGO	240 mA h g^{-1} at 0.1 A g^{-1}, with a 68% capacity retain at 1 A g^{-1} after 1000 cycles	[62] Electrochim. Acta, 2022, 411, 140070
T-$Nb_2O_{5-x}F_y$-C-NBs	292 mA h g^{-1} at 0.05 A g^{-1}, 0.002% capacity decay per cycle over 10,000 cycles at 1 A g^{-1}	[47] J. Mater. Chem. A, 2019, 7, 20813

Table 2. *Cont.*

Materials	Sodium Storage Performances	References
black Nb_2O_{5-x}@rGO	202 and 123 mA h g^{-1} at 500 and 3000 mA g^{-1}, respectively.	[80] Small, 2019, 15, 1901272
meso-Nb_2O_5@C	133.4 mA h g^{-1} at 50C, 112.4 mA h g^{-1} (80.5% retention) after 10,000 cycles even at 20 C	[73] J. Mater. Chem. A, 2022, 10, 11470
Nb_2O_{5-x}@MEC	105 mA h g^{-1} at 20 A g^{-1} with stable Coulombic efficiency of nearly 100% after 5000 cycles	[79] Adv. Energy Mater., 2022, 12, 2103716
CNT@T-Nb_2O_5@C	Areal capacities of 2.7 mA h cm^{-2} after 200 cycles at the mass loading of 16.6 mg cm^{-2}	[81] Nano Energy, 2020, 78, 105265
(m-Nb_2O_5)/CNF	287 mA h g^{-1} and 172 mA h g^{-1} at the rate of 0.5 C and 150 C, respectively	[86] Small, 2019, 15, 1804539
(NS-TiO_2)	307.5 and 156.4 mA h g^{-1} at 33.5 and 5025 mA g^{-1}, respectively, and 90.5% retention over 2400 cycles at 3350 mA g^{-1}	[95] Adv. Energy Mater., 2021, 11, 2003037
TiO_2/C	262 and 97 mA h g^{-1} at 0.1 and 2.0 A g^{-1}, respectively, and ~109 mA h g^{-1} over 1000 cycles at 1.0 A g^{-1}	[96] ACS Appl. Energy Mater., 2022, 5, 3447
$Na_2Ti_3O_7$@C	173 mA h g^{-1} at 200 mA g^{-1} and only 0.026% attenuation per cycle at 2 A g^{-1} after 200 cycles	[97] Chem. Eng. J., 2019, 378, 122209
nCNT@$Na_2Ti_3O_7$	206.5 mA h g^{-1} at 0.1 A g^{-1}, and ~93% capacity retention after 1000 cycles at 5 A g^{-1})	[98] Nanoscale, 2022, 14, 8374

5. Conclusions and Perspectives

As a typical representative of niobium-based oxides used as anodes in secondary battery applications, Nb_2O_5 has received extensive attention due to its inherent structural energy storage advantages. The 4g layer in its structure has a spacious atom holding space, which can provide a preferred storage and transport place for ions, forming a quasi-2D channel for sodium ion transport. In addition, due to its rich redox chemistry and high chemical structure stability, it shows excellent rate and cycle stability performance in SIBs. However, the poor electronic conductivity hinders its application in electrochemical energy storage. Although the sodium storage performance of Nb_2O_5 electrode can be improved through various strategies, such as structure optimization and electronic conductivity improvement engineering, there are still some important problems that need to be clarified and solved so that they can be applied to large-scale energy storage and smart grids based on their cost advantages in the future.

There are many researches on theoretical calculation of Nb_2O_5 in LIBs, but few in SIBs. Although it has the large interplanar spacing of 0.39 nm for the (001) planes, it is necessary to calculate the spatial steric resistance, migration path and barrier range of sodium ions due to its larger Na-ion radius after they are embedded. In the future, more theoretical calculation research should focus on the Na-ion insertion/extraction process, as well as dendrites and side reactions in SIBs.

Although Nb_2O_5 has many advantages in sodium storage, it also has some disadvantages. Its poor electronic conductivity restricts its structural energy storage advantages. Compared with the conversion-type and alloy-type sodium storage anodes, its theoretical specific capacity is relatively lower, which further limits its practical application. How to significantly improve the electronic conductivity of Nb_2O_5 through effective strategies is still the key research direction in the future. Among them, carbon modification, structural optimization and defect engineering are still the main modification methods. Although a nano-sized electrode is conducive to enhance its electrochemical sodium storage performance, it also brings additional and complex synthesis processes, low tap density and difficulties in commercial batch production. The development and application of micron-sized electrodes will be an important research topic in the future. In addition, during the process of carbon modification, the mass percentage of carbon material is often high.

Although more carbon can bring better electronic conductivity, its sodium storage capacity is low, which will further reduce the sodium storage capacity of the whole Nb_2O_5-based electrode. Developing low-carbon modification projects, which can still significantly improve their electronic conductivity, will be the focus of carbon modification strategies in the future.

For the practical application of Nb_2O_5 anodes, at present, most of the modified preparation methods are complex, with many preparation processes, expensive reaction materials, harsh conditions, expensive equipment, etc., which are not conducive to their large-scale preparation and application. In the future, the modification strategy should focus on the simple and easy methods for large-area preparation. In addition, high- and low-temperature research on Nb_2O_5 electrodes and the synergistic effect of composite electrodes are all worthy of study in the future.

References

1. Omer, A.M. Energy, environment and sustainable development. *Renew. Sustain. Energy Rev.* **2008**, *12*, 2265–2300. [CrossRef]
2. Midilli, A.; Dincer, I.; Ay, M. Green energy strategies for sustainable development. *Energy Policy* **2006**, *34*, 3623–3633. [CrossRef]
3. Rahman, A.; Farrok, O.; Haque, M.M. Environmental impact of renewable energy source based electrical power plants: Solar, wind, hydroelectric, biomass, geothermal, tidal, ocean, and osmotic. *Renew. Sustain. Energy Rev.* **2022**, *161*, 492–505. [CrossRef]
4. Yu, Y.; Lee, S.J.; Theerthagiri, J.; Lee, Y.; Choi, M.Y. Architecting the AuPt alloys for hydrazine oxidation as an anolyte in fuel cell: Comparative analysis of hydrazine splitting and water splitting for energy-saving H-2 generation. *Appl. Catal. B* **2022**, *316*, 121603. [CrossRef]
5. Iqbal, K.; Ikram, M.; Afzal, M.; Ali, S. Efficient, low-dimensional nanocomposite bilayer CuO/ZnO solar cell at various annealing temperatures. *Mater. Renew. Sustain. Energy* **2018**, *7*, 4. [CrossRef]
6. Ikram, M.; Murray, R.; Imran, M.; Ali, S.; Shah, S.I. Enhanced performance of P3HT/(PCBM:ZnO:TiO$_2$) blend based hybrid organic solar cells. *Mater. Res. Bull.* **2016**, *75*, 35–40. [CrossRef]
7. Hall, P.J.; Bain, E.J. Energy-storage technologies and electricity generation. *Energy Policy* **2008**, *36*, 4352–4355. [CrossRef]
8. Arico, A.S.; Bruce, P.; Scrosati, B.; Tarascon, J.M.; Van Schalkwijk, W. Nanostructured materials for advanced energy conversion and storage devices. *Nat. Mater.* **2005**, *4*, 366–377. [CrossRef]
9. Larcher, D.; Tarascon, J.M. Towards greener and more sustainable batteries for electrical energy storage. *Nat. Chem.* **2015**, *7*, 19–29. [CrossRef]
10. Goodenough, J.B.; Kim, Y. Challenges for Rechargeable Li Batteries. *Chem. Mater.* **2010**, *22*, 587–603. [CrossRef]
11. Dunn, B.; Kamath, H.; Tarascon, J.-M. Electrical Energy Storage for the Grid: A Battery of Choices. *Science* **2011**, *334*, 928–935. [CrossRef] [PubMed]
12. Li, M.; Lu, J.; Chen, Z.; Amine, K. 30 Years of Lithium-Ion Batteries. *Adv. Mater.* **2018**, *30*, 1800561. [CrossRef]
13. Ji, L.; Lin, Z.; Alcoutlabi, M.; Zhang, X. Recent developments in nanostructured anode materials for rechargeable lithium-ion batteries. *Energy Environ. Sci.* **2011**, *4*, 2682–2699. [CrossRef]
14. Lu, L.; Han, X.; Li, J.; Hua, J.; Ouyang, M. A review on the key issues for lithium-ion battery management in electric vehicles. *J. Power Source* **2013**, *226*, 272–288. [CrossRef]
15. Huang, B.; Pan, Z.; Su, X.; An, L. Recycling of lithium-ion batteries: Recent advances and perspectives. *J. Power Source* **2018**, *399*, 274–286. [CrossRef]
16. Yabuuchi, N.; Kubota, K.; Dahbi, M.; Komaba, S. Research Development on Sodium-Ion Batteries. *Chem. Rev.* **2014**, *114*, 11636–11682. [CrossRef] [PubMed]
17. Nayak, P.K.; Yang, L.; Brehm, W.; Adelhelm, P. From Lithium-Ion to Sodium-Ion Batteries: Advantages, Challenges, and Surprises. *Angew. Chem. Int. Ed.* **2018**, *57*, 102–120. [CrossRef]

18. Kim, S.-W.; Seo, D.-H.; Ma, X.; Ceder, G.; Kang, K. Electrode Materials for Rechargeable Sodium-Ion Batteries: Potential Alternatives to Current Lithium-Ion Batteries. *Adv. Energy Mater.* **2012**, *2*, 710–721. [CrossRef]
19. Hwang, J.-Y.; Myung, S.-T.; Sun, Y.-K. Sodium-ion batteries: Present and future. *Chem. Soc. Rev.* **2017**, *46*, 3529–3614. [CrossRef]
20. Delmas, C. Sodium and Sodium-Ion Batteries: 50 Years of Research. *Adv. Energy Mater.* **2018**, *8*, 1703137. [CrossRef]
21. Li, L.; Zheng, Y.; Zhang, S.; Yang, J.; Shao, Z.; Guo, Z. Recent progress on sodium ion batteries: Potential high-performance anodes. *Energy Environ. Sci.* **2018**, *11*, 2310–2340. [CrossRef]
22. Xiang, X.; Zhang, K.; Chen, J. Recent Advances and Prospects of Cathode Materials for Sodium-Ion Batteries. *Adv. Mater.* **2015**, *27*, 5343–5364. [CrossRef] [PubMed]
23. Deng, Q. Advanced Materials for Electrocatalysis and Energy Storage. *Coatings* **2022**, *12*, 901. [CrossRef]
24. Lao, M.; Zhang, Y.; Luo, W.; Yan, Q.; Sun, W.; Dou, S.X. Alloy-Based Anode Materials toward Advanced Sodium-Ion Batteries. *Adv. Mater.* **2017**, *29*, 1700622. [CrossRef] [PubMed]
25. Deng, X.; Chen, Z.; Cao, Y. Transition metal oxides based on conversion reaction for sodium-ion battery anodes. *Mater. Today Chem.* **2018**, *9*, 114–132. [CrossRef]
26. Liu, Z.-G.; Du, R.; He, X.-X.; Wang, J.-C.; Qiao, Y.; Li, L.; Chou, S.-L. Recent Progress on Intercalation-Based Anode Materials for Low-Cost Sodium-Ion Batteries. *ChemSusChem* **2021**, *14*, 3724–3743. [CrossRef]
27. Tan, H.; Chen, D.; Rui, X.; Yu, Y. Peering into Alloy Anodes for Sodium-Ion Batteries: Current Trends, Challenges, and Opportunities. *Adv. Funct. Mater.* **2019**, *29*, 1808745. [CrossRef]
28. Liu, Y.; Zhang, N.; Jiao, L.; Tao, Z.; Chen, J. Ultrasmall Sn Nanoparticles Embedded in Carbon as High-Performance Anode for Sodium-Ion Batteries. *Adv. Funct. Mater.* **2015**, *25*, 214–220. [CrossRef]
29. Liu, Z.; Yu, X.-Y.; Lou, X.W.; Paik, U. Sb@C coaxial nanotubes as a superior long-life and high-rate anode for sodium ion batteries. *Energy Environ. Sci.* **2016**, *9*, 2314–2318. [CrossRef]
30. Zhang, H.; Hasa, I.; Passerini, S. Beyond Insertion for Na-Ion Batteries: Nanostructured Alloying and Conversion Anode Materials. *Adv. Energy Mater.* **2018**, *8*, 1702582. [CrossRef]
31. Fang, L.; Bahlawane, N.; Sun, W.; Pan, H.; Xu, B.B.; Yan, M.; Jiang, Y. Conversion-Alloying Anode Materials for Sodium Ion Batteries. *Small* **2021**, *17*, 2101137. [CrossRef] [PubMed]
32. Wei, X.; Wang, X.; Tan, X.; An, Q.; Mai, L. Nanostructured Conversion-Type Negative Electrode Materials for Low-Cost and High-Performance Sodium-Ion Batteries. *Adv. Funct. Mater.* **2018**, *28*, 1804458. [CrossRef]
33. Xu, Z.-L.; Park, J.; Yoon, C.; Kim, H.; Kang, K. Graphitic Carbon Materials for Advanced Sodium-Ion Batteries. *Small Methods* **2019**, *3*, 1800227. [CrossRef]
34. Hou, H.; Qiu, X.; Wei, W.; Zhang, Y.; Ji, X. Carbon Anode Materials for Advanced Sodium-Ion Batteries. *Adv. Energy Mater.* **2017**, *7*, 1602898. [CrossRef]
35. Lee, S.J.; Theerthagiri, J.; Nithyadharseni, P.; Arunachalam, P.; Balaji, D.; Kumar, A.M.; Madhavan, J.; Mittal, V.; Choi, M.Y. Heteroatom-doped graphene-based materials for sustainable energy applications: A review. *Renew. Sustain. Energy Rev.* **2021**, *143*, 110849. [CrossRef]
36. Pan, H.; Lu, X.; Yu, X.; Hu, Y.-S.; Li, H.; Yang, X.-Q.; Chen, L. Sodium Storage and Transport Properties in Layered $Na_2Ti_3O_7$ for Room-Temperature Sodium-Ion Batteries. *Adv. Energy Mater.* **2013**, *3*, 1186–1194. [CrossRef]
37. Lou, S.; Zhao, Y.; Wang, J.; Yin, G.; Du, C.; Sun, X. Ti-Based Oxide Anode Materials for Advanced Electrochemical Energy Storage: Lithium/Sodium Ion Batteries and Hybrid Pseudocapacitors. *Small* **2019**, *15*, 1904740. [CrossRef]
38. Deng, Q.; Fu, Y.; Zhu, C.; Yu, Y. Niobium-Based Oxides Toward Advanced Electrochemical Energy Storage: Recent Advances and Challenges. *Small* **2019**, *15*, 1804884. [CrossRef] [PubMed]
39. Wang, H.; Qian, R.; Cheng, Y.; Wu, H.-H.; Wu, X.; Pan, K.; Zhang, Q. Micro/nanostructured $TiNb_2O_7$-related electrode materials for high-performance electrochemical energy storage: Recent advances and future prospects. *J. Mater. Chem. A* **2020**, *8*, 18425–18463. [CrossRef]
40. Shen, L.; Wang, Y.; Lv, H.; Chen, S.; van Aken, P.A.; Wu, X.; Maier, J.; Yu, Y. Ultrathin $Ti_2Nb_2O_9$ Nanosheets with Pseudocapacitive Properties as Superior Anode for Sodium-Ion Batteries. *Adv. Mater.* **2018**, *30*, 1804378. [CrossRef] [PubMed]
41. Lim, E.; Jo, C.; Kim, M.S.; Kim, M.-H.; Chun, J.; Kim, H.; Park, J.; Roh, K.C.; Kang, K.; Yoon, S.; et al. High-Performance Sodium-Ion Hybrid Supercapacitor Based on Nb_2O_5@Carbon Core-Shell Nanoparticles and Reduced Graphene Oxide Nanocomposites. *Adv. Funct. Mater.* **2016**, *26*, 3711–3719. [CrossRef]
42. Yi, T.-F.; Sari, H.M.K.; Li, X.; Wang, F.; Zhu, Y.-R.; Hu, J.; Zhang, J.; Li, X. A review of niobium oxides based nanocomposites for lithium-ion batteries, sodium-ion batteries and supercapacitors. *Nano Energy* **2021**, *85*, 105955. [CrossRef]
43. Sun, H.; Mei, L.; Liang, J.; Zhao, Z.; Lee, C.; Fei, H.; Ding, M.; Lau, J.; Li, M.; Wang, C.; et al. Three-dimensional holey-graphene/niobia composite architectures for ultrahigh-rate energy storage. *Science* **2017**, *356*, 599–604. [CrossRef] [PubMed]
44. Deng, Q.; Li, M.; Wang, J.; Jiang, K.; Hu, Z.; Chu, J. Free-anchored Nb_2O_5@graphene networks for ultrafast-stable lithium storage. *Nanotechnology* **2018**, *29*, 185401. [CrossRef]
45. Jing, P.; Liu, K.; Soule, L.; Wang, J.; Li, T.; Zhao, B.; Liu, M. Engineering the architecture and oxygen deficiency of T-Nb_2O_5-carbon-graphene composite for high-rate lithium-ion batteries. *Nano Energy* **2021**, *89*, 106398. [CrossRef]
46. Griffith, K.J.; Forse, A.C.; Griffin, J.M.; Grey, C.P. High-Rate Intercalation without Nanostructuring in Metastable Nb_2O_5 Bronze Phases. *J. Am. Chem. Soc.* **2016**, *138*, 8888–8899. [CrossRef]

47. Wu, Y.; Fan, X.; Chen, Y.; Gaddam, R.R.; Yu, F.; Xiao, C.; Lin, C.; Zhao, Q.; Sun, X.; Wang, H.; et al. Fluorine substitution enabling pseudocapacitive intercalation of sodium ions in niobium oxyfluoride. *J. Mater. Chem. A* **2019**, *7*, 20813–20823. [CrossRef]

48. Chen, D.; Wang, J.-H.; Chou, T.-F.; Zhao, B.; El-Sayed, M.A.; Liu, M. Unraveling the Nature of Anomalously Fast Energy Storage in T-Nb$_2$O$_5$. *J. Am. Chem. Soc.* **2017**, *139*, 7071–7081. [CrossRef]

49. Augustyn, V.; Come, J.; Lowe, M.A.; Kim, J.W.; Taberna, P.-L.; Tolbert, S.H.; Abruna, H.D.; Simon, P.; Dunn, B. High-rate electrochemical energy storage through Li+ intercalation pseudocapacitance. *Nat. Mater.* **2013**, *12*, 518–522. [CrossRef]

50. Augustyn, V.; Simon, P.; Dunn, B. Pseudocapacitive oxide materials for high-rate electrochemical energy storage. *Energy Environ. Sci.* **2014**, *7*, 1597–1614. [CrossRef]

51. Wei, Q.; DeBlock, R.H.; Butts, D.M.; Choi, C.; Dunn, B. Pseudocapacitive Vanadium-based Materials toward High-Rate Sodium-Ion Storage. *Energy Environ. Mater.* **2020**, *3*, 221–234. [CrossRef]

52. Yu, F.; Huang, T.; Zhang, P.; Tao, Y.; Cui, F.-Z.; Xie, Q.; Yao, S.; Wang, F. Design and synthesis of electrode materials with both battery-type and capacitive charge storage. *Energy Storage Mater.* **2019**, *22*, 235–255. [CrossRef]

53. Jiang, Y.; Liu, J. Definitions of Pseudocapacitive Materials: A Brief Review. *Energy Environ. Mater.* **2019**, *2*, 30–37. [CrossRef]

54. Choi, C.; Ashby, D.S.; Butts, D.M.; DeBlock, R.H.; Wei, Q.; Lau, J.; Dunn, B. Achieving high energy density and high power density with pseudocapacitive materials. *Nat. Rev. Mater.* **2020**, *5*, 5–19. [CrossRef]

55. Lukatskaya, M.R.; Kota, S.; Lin, Z.; Zhao, M.-Q.; Shpigel, N.; Levi, M.D.; Halim, J.; Taberna, P.-L.; Barsoum, M.; Simon, P.; et al. Ultra-high-rate pseudocapacitive energy storage in two-dimensional transition metal carbides. *Nat. Energy* **2017**, *2*, 17105. [CrossRef]

56. Xu, G.; Wang, Q.; Su, Y.; Liu, M.; Li, Q.; Zhang, Y. Revealing Electrochemical Sodiation Mechanism of Orthogonal-Nb$_2$O$_5$ Nanosheets by In Situ Transmission Electron Microscopy. *Acta Phys.-Chim. Sin.* **2022**, *38*, 2009073.

57. Ni, J.; Wang, W.; Wu, C.; Liang, H.; Maier, J.; Yu, Y.; Li, L. Highly Reversible and Durable Na Storage in Niobium Pentoxide through Optimizing Structure, Composition, and Nanoarchitecture. *Adv. Mater.* **2017**, *29*, 1605607. [CrossRef]

58. Yang, L.; Zhu, Y.-E.; Sheng, J.; Li, F.; Tang, B.; Zhang, Y.; Zhou, Z. T-Nb$_2$O$_5$/C Nanofibers Prepared through Electrospinning with Prolonged Cycle Durability for High-Rate Sodium-Ion Batteries Induced by Pseudocapacitance. *Small* **2017**, *13*, 1702588. [CrossRef]

59. Yan, L.; Chen, G.; Sarker, S.; Richins, S.; Wang, H.; Xu, W.; Rui, X.; Luo, H. Ultrafine Nb$_2$O$_5$ Nanocrystal Coating on Reduced Graphene Oxide as Anode Material for High Performance Sodium Ion Battery. *ACS Appl. Mater. Interfaces* **2016**, *8*, 22213–22219. [CrossRef]

60. Wang, L.; Bi, X.; Yang, S. Partially Single-Crystalline Mesoporous Nb$_2$O$_5$ Nanosheets in between Graphene for Ultrafast Sodium Storage. *Adv. Mater.* **2016**, *28*, 7672–7679. [CrossRef]

61. Li, H.; Zhu, Y.; Dong, S.; Shen, L.; Chen, Z.; Zhang, X.; Yu, G. Self-Assembled Nb$_2$O$_5$ Nanosheets for High Energy-High Power Sodium Ion Capacitors. *Chem. Mater.* **2016**, *28*, 5753–5760. [CrossRef]

62. Bi, Z.; Zhang, Y.; Li, X.; Liang, Y.; Ma, W.; Zhou, Z.; Zhu, M. Porous fibers of carbon decorated T-Nb$_2$O$_5$ nanocrystal anchored on three-dimensional rGO composites combined with rGO nanosheets as an anode for high-performance flexible sodium-ion capacitors. *Electrochim. Acta* **2022**, *411*, 140070. [CrossRef]

63. Zhao, Z.; Cheng, J.; Li, K.; Li, C.; Zhang, S.; Pei, X.; Niu, Z.; Liu, Z.; Fu, Y.; Li, D. Heterojunction interfacial promotion of fast and prolonged alkali-ion storage of urchin-like Nb$_2$O$_5$@C nanospheres. *J. Mater. Chem. A* **2021**, *9*, 23467–23476. [CrossRef]

64. Chen, Z.; Chen, W.; Wang, H.; Xiao, Z.; Yu, F. N-doped carbon-coated ultrasmall Nb$_2$O$_5$ nanocomposite with excellent long cyclability for sodium storage. *Nanoscale* **2020**, *12*, 18673–18681. [CrossRef] [PubMed]

65. Tong, Z.; Liu, S.; Zhou, Y.; Zhao, J.; Wu, Y.; Wang, Y.; Li, Y. Rapid redox kinetics in uniform sandwich-structured mesoporous Nb$_2$O$_5$/graphene/mesoporous Nb$_2$O$_5$ nanosheets for high-performance sodium-ion supercapacitors. *Energy Storage Mater.* **2018**, *13*, 223–232. [CrossRef]

66. Wang, X.; Li, Q.; Zhang, L.; Hu, Z.; Yu, L.; Jiang, T.; Lu, C.; Yan, C.; Sun, J.; Liu, Z. Caging Nb$_2$O$_5$ Nanowires in PECVD-Derived Graphene Capsules toward Bendable Sodium-Ion Hybrid Supercapacitors. *Adv. Mater.* **2018**, *30*, 1800963. [CrossRef]

67. Liu, F.; Cheng, X.; Xu, R.; Wu, Y.; Jiang, Y.; Yu, Y. Binding Sulfur-Doped Nb$_2$O$_5$ Hollow Nanospheres on Sulfur-Doped Graphene Networks for Highly Reversible Sodium Storage. *Adv. Funct. Mater.* **2018**, *28*, 1800394. [CrossRef]

68. She, L.; Iran, Z.; Kang, L.; He, X.; Lei, Z.; Shi, F.; Xu, H.; Sun, J.; Liu, Z.-H. Nb$_2$O$_5$ Nanoparticles Anchored on an N-Doped Graphene Hybrid Anode for a Sodium-Ion Capacitor with High Energy Density. *ACS Omega* **2018**, *3*, 15943–15951. [CrossRef]

69. Zhu, S.; Yang, Y.; Liu, J.; Sun, J. Carbon-confined ultrasmall T-Nb$_2$O$_5$ nanocrystals anchored on carbon nanotubes by pyrolysing MLD-niobiumcone films for enhanced electrochemical applications. *J. Mater. Chem. A* **2020**, *8*, 25371–25381. [CrossRef]

70. Wu, Y.; Fan, X.; Gaddam, R.R.; Zhao, Q.; Yang, D.; Sun, X.; Wang, C.; Zhao, X.S. Mesoporous niobium pentoxide/carbon composite electrodes for sodium-ion capacitors. *J. Power Source* **2018**, *408*, 82–90. [CrossRef]

71. Yuan, J.; Li, X.; Liu, J.; Zuo, S.; Li, X.; Li, F.; Gan, Y.; He, H.; Xu, X.; Zhang, X.; et al. Pomegranate-like structured Nb$_2$O$_5$/Carbon@N-doped carbon composites as ultrastable anode for advanced sodium/potassium-ion batteries. *J. Colloid Interface Sci.* **2022**, *613*, 84–93. [CrossRef] [PubMed]

72. Subramanian, Y.; Veerasubramani, G.K.; Park, M.-S.; Kim, D.-W. Core-shell structured Nb$_2$O$_5$@N-doped carbon nanoparticles as an anode material for Na-ion batteries. *Mater. Lett.* **2022**, *314*, 131891. [CrossRef]

73. Jiang, Y.; Guo, S.; Li, Y.; Hu, X. Rapid microwave synthesis of carbon-bridged Nb$_2$O$_5$ mesocrystals for high-energy and high-power sodium-ion capacitors. *J. Mater. Chem. A* **2022**, *10*, 11470–11476. [CrossRef]

74. Zhang, X.; Wang, J.; Wang, X.; Li, Y.; Zhao, Y.; Bakenov, Z.; Li, G. 3D ordered macroporous amorphous Nb_2O_5 as anode material for high-performance sodium-ion batteries. *Appl. Surf. Sci.* **2021**, *567*, 150862. [CrossRef]

75. Jin, J.; Cai, J.; Wang, X.; Sun, Z.; Song, Y.; Sun, J. Architecturing aligned orthorhombic Nb_2O_5 nanowires toward sodium-ion hybrid capacitor and Lithium-Sulfur battery applications. *Flatchem* **2021**, *27*, 100236. [CrossRef]

76. Lian, Y.; Yang, N.; Bai, Y.; Wang, D.; Yan, H.; Wang, Z.; Zhao, J.; Zhang, H. Nb_2O_5 quantum dots confined in multi-chamber yeast carbon for sodium ion hybrid capacitors. *J. Alloys Compd.* **2022**, *896*, 163128. [CrossRef]

77. Huang, H.; Xu, R.; Feng, Y.; Zeng, S.; Jiang, Y.; Wang, H.; Luo, W.; Yu, Y. Sodium/Potassium-Ion Batteries: Boosting the Rate Capability and Cycle Life by Combining Morphology, Defect and Structure Engineering. *Adv. Mater.* **2020**, *32*, 1904320. [CrossRef]

78. Yang, Z.; Zhu, L.; Lv, C.; Zhang, R.; Wang, H.; Wang, J.; Zhang, Q. Defect engineering of molybdenum disulfide for energy storage. *Mater. Chem. Front.* **2021**, *5*, 5880–5896. [CrossRef]

79. Luo, D.; Ma, C.; Hou, J.; Zhang, Z.; Feng, R.; Yang, L.; Zhang, X.; Lu, H.; Liu, J.; Li, Y.; et al. Integrating Nanoreactor with O-Nb-C Heterointerface Design and Defects Engineering Toward High-Efficiency and Longevous Sodium Ion Battery. *Adv. Energy Mater.* **2022**, *12*, 2103716. [CrossRef]

80. Tong, Z.; Yang, R.; Wu, S.; Shen, D.; Jiao, T.; Zhang, K.; Zhang, W.; Lee, C.-S. Surface-Engineered Black Niobium Oxide@Graphene Nanosheets for High-Performance Sodium-/Potassium-Ion Full Batteries. *Small* **2019**, *15*, 1901272. [CrossRef]

81. Chen, Y.; Yousaf, M.; Wang, Y.; Wang, Z.; Lou, S.; Han, R.P.S.; Yang, Y.; Cao, A. Nanocable with thick active intermediate layer for stable and high-areal-capacity sodium storage. *Nano Energy* **2020**, *78*, 105265. [CrossRef]

82. Hashemi, S.A.; Ramakrishna, S.; Aberle, A.G. Recent progress in flexible-wearable solar cells for self-powered electronic devices. *Energy Environ. Sci.* **2020**, *13*, 685–743. [CrossRef]

83. Wang, J.-L.; Hassan, M.; Liu, J.-W.; Yu, S.-H. Nanowire Assemblies for Flexible Electronic Devices: Recent Advances and Perspectives. *Adv. Mater.* **2018**, *30*, 1803430. [CrossRef] [PubMed]

84. Choi, S.; Lee, H.; Ghaffari, R.; Hyeon, T.; Kim, D.-H. Recent Advances in Flexible and Stretchable Bio-Electronic Devices Integrated with Nanomaterials. *Adv. Mater.* **2016**, *28*, 4203–4218. [CrossRef]

85. Xu, Y.; Zhu, Y.; Han, F.; Luo, C.; Wang, C. 3D Si/C Fiber Paper Electrodes Fabricated Using a Combined Electro-spray/Electrospinning Technique for Li-Ion Batteries. *Adv. Energy Mater.* **2015**, *5*, 1400753. [CrossRef]

86. Li, Y.; Wang, H.; Wang, L.; Mao, Z.; Wang, R.; He, B.; Gong, Y.; Hu, X. Mesopore-Induced Ultrafast Na+-Storage in T-Nb_2O_5/Carbon Nanofiber Films toward Flexible High-Power Na-Ion Capacitors. *Small* **2019**, *15*, 1804539. [CrossRef]

87. She, L.; Zhang, F.; Jia, C.; Kang, L.; Li, Q.; He, X.; Sun, J.; Lei, Z.; Liu, Z.-H. Electrospun Nb_2O_5 nanorods/microporous multichannel carbon nanofiber film anode for Na+ ion capacitors with good performance. *J. Colloid Interface Sci.* **2020**, *573*, 1–10. [CrossRef]

88. Jia, R.; Jiang, Y.; Li, R.; Chai, R.; Lou, Z.; Shen, G.; Chen, D. Nb_2O_5 nanotubes on carbon cloth for high performance sodiumion capacitors. *Sci. China Mater.* **2020**, *63*, 1171–1181. [CrossRef]

89. Kang, J.; Zhang, H.; Zhan, Z.; Li, Y.; Ling, M.; Gao, X. Construction of a Flexible Nb_2O_5/Carboxyl Multiwalled Carbon Nanotube Film as Anode for Lithium and Sodium Storages. *ACS Appl. Energy Mater.* **2020**, *3*, 11841–11847. [CrossRef]

90. Real, C.G.; Thaines, E.H.N.S.; Pocrifka, L.A.; Freitas, R.G.; Singh, G.; Zanin, H. Freestanding niobium pentoxide-decorated multiwalled carbon nanotube electrode: Charge storage mechanism in sodium-ion pseudocapacitor and battery. *J. Energy Storage* **2022**, *52*, 104793. [CrossRef]

91. Yang, H.; Xu, R.; Gong, Y.; Yao, Y.; Gu, L.; Yu, Y. An interpenetrating 3D porous reticular Nb_2O_5@carbon thin film for superior sodium storage. *Nano Energy* **2018**, *48*, 448–455. [CrossRef]

92. Wang, H.-G.; Li, W.; Liu, D.-P.; Feng, X.-L.; Wang, J.; Yang, X.-Y.; Zhang, X.-b.; Zhu, Y.; Zhang, Y. Flexible Electrodes for Sodium-Ion Batteries: Recent Progress and Perspectives. *Adv. Mater.* **2017**, *29*, 1703012. [CrossRef] [PubMed]

93. Deng, Q.; Chen, F.; Liu, S.; Bayaguud, A.; Feng, Y.; Zhang, Z.; Fu, Y.; Yu, Y.; Zhu, C. Advantageous Functional Integration of Adsorption-Intercalation-Conversion Hybrid Mechanisms in 3D Flexible Nb_2O_5@Hard Carbon@MoS_2@Soft Carbon Fiber Paper Anodes for Ultrafast and Super-Stable Sodium Storage. *Adv. Funct. Mater.* **2020**, *30*, 1908665. [CrossRef]

94. Wang, L.; Bi, X.; Yang, S. Synergic antimony-niobium pentoxide nanomeshes for high-rate sodium storage. *J. Mater. Chem. A* **2018**, *6*, 6225–6232. [CrossRef]

95. Fan, M.; Lin, Z.; Zhang, P.; Ma, X.; Wu, K.; Liu, M.; Xiong, X. Synergistic Effect of Nitrogen and Sulfur Dual-Doping Endows TiO_2 with Exceptional Sodium Storage Performance. *Adv. Energy Mater.* **2021**, *11*, 2003037. [CrossRef]

96. Huo, J.; Ren, Y.; Zhang, G.; Wang, X.; Guo, S. Boosting Sodium Storage of Hierarchical Nanofibers with Porous Carbon-Supported Anatase TiO_2/TiO_2(B) Nanowires. *ACS Appl. Energy Mater.* **2022**, *5*, 3447–3453. [CrossRef]

97. Zhong, W.; Tao, M.; Tang, W.; Gao, W.; Yang, T.; Zhang, Y.; Zhan, R.; Bao, S.-J.; Xu, M. MXene-derivative pompon-like $Na_2Ti_3O_7$@C anode material for advanced sodium ion batteries. *Chem. Eng. J.* **2019**, *378*, 122209. [CrossRef]

98. Chen, J.; Mu, H.; Ding, J.; Zhang, Y.; Wang, W.; Wang, G. Stretchable sodium-ion capacitors based on coaxial CNT supported $Na_2Ti_3O_7$ with high capacitance contribution. *Nanoscale* **2022**, *14*, 8374–8384. [CrossRef]